Ecological Modelling 273 (2014) 210–219

Contents lists available at ScienceDirect

Ecological Modelling

journal homepage: www.elsevier.com/locate/ecolmodel

# Relative branch size in branch clusters modelled through a Markovian process

A. Zubizarreta-Gerendiain[a,b], M.P. Fernández[c,*]

[a] School of Forest Sciences, University of Eastern Finland, Yliopistokatu 7, Borealis Building, Joensuu, Finland
[b] Forest Research Center, School of Agriculture, University of Lisbon, Tapada da Ajuda, Lisboa 1349-017, Portugal
[c] Department of Ecosystems and Environment, Faculty of Agriculture and Forest Engineering, Pontificia Universidad Católica de Chile, Av. Vicuña Mackenna 4860, Macul, 7820436 Santiago, Chile

ARTICLE INFO

*Article history:*
Received 17 May 2013
Received in revised form 5 November 2013
Accepted 11 November 2013
Available online 5 December 2013

*Keywords:*
Branching
Markov process
Stochastic modelling
Acrotony
*Pinus radiata*

ABSTRACT

Information on tree canopy architecture is crucial in forestry practice because the quality and price of standing trees and final logs directly depend on it. Simultaneously, accurate empirical or functional–structural models require information based on field observations. *Pinus radiata* is a polycyclic species that follows an acrotony law when forming a new branch cluster, showing smaller branches in its base and larger ones at the top of a forming cluster. The objective of this study was to describe the acrotony of the branches in a branch cluster as a Markov chain. Markov chains represent stochastic processes in discrete time that undergo a transition from one state to another among a finite number of possible states. The probability of transition from state $i$ to a state $j$ depends only on the current state, $i$. For modelling acrotony, the relative vigour (expressed as relative branch diameter in relation to the largest one) of each branch was selected as the stochastic variable and the states corresponded to five possible relative size ranges.

The branches observed within a *P. radiata* cluster were ordered following their relative sizes (from largest to smallest), and Markovian transition matrixes were calculated for each branch cluster (whorls of 3–12 branches). The transition matrixes were defined as the probabilities of one branch being followed by an equal-sized or smaller branch when observing the cluster from the top down. The obtained Markov chain matrixes were used in a stochastic data simulation, which was validated with an independent dataset. The presented matrixes can be incorporated into traditional simulation models or functional–structural models. The validation results show that the proposed methodology accurately reflects the variability of the branch sizes in a cluster, and we suggest its application to other species that display a clustered organisation of branches.



## 1. Introduction

The value of the wood as a raw material is affected by its quantity as well as it quality. While the quantity is a relatively easy parameter to measure, quality is more difficult (e.g., it changes depending on the industry). So it is important to study the tree raw material, on one hand by the stem diameter/volume and on the other hand by the potential quality of sawn timber (e.g., branch characteristics and knot locations, sizes and numbers). The quality and price of standing trees and final logs directly depend on tree structures. Thus, information on the architecture of the canopy, i.e., on branch numbers, sizes and positions, is crucial in forestry practice because branches become knots, which are internal defects of the wood that directly decrease the mechanical properties of it, as well as aesthetic aspects of the final products. Therefore the capacity to predict the quality and value of forest products is necessary to improve the wood supply chain. For instance, there are several studies (e.g., Grace et al., 1998; Todoroki et al., 2001) that consider the diameter of the largest branch in a cluster to be an important parameter to take into account when referring to wood quality.

The architecture of a plant depends on the nature and relative placement of each of its parts, which at any given time arises from the balance between the expression of the endogenous growth process and exogenous constraints conferred by the environment. The concept of a balanced structural component for predicting growth allocation in the structures of trees has been widely studied (e.g., Mäkelä et al., 2002; Mäkelä, 2012). Thus, the objective of the architectural analysis of a tree is, in general, to identify these endogenous processes through observation (Barthélémy, 2003; Barthélémy and

* Corresponding author. Tel.: +56 2 2 354 4884.
*E-mail addresses:* ane.zubizarreta@uef.fi (A. Zubizarreta-Gerendiain), pfernan@uc.cl, mpfq15@gmail.com (M.P. Fernández).

0304-3800/$ – see front matter © 2013 Elsevier B.V. All rights reserved.
http://dx.doi.org/10.1016/j.ecolmodel.2013.11.012

Caraglio, 2007). Within this context, modelling of tree knots based on branch data is an important aspect.

Tree and wood modelling involves increasing quality parameters to support forestry decision-making systems related to the quantity and quality of products. For these purposes, functional-structural models, which require information based on observed allometric relationships are useful. Modelling of forest tree allometry has many applications, from understanding physiological relationships (e.g., the allometry between sapwood and leaf area, Monserud and Marshall, 1999) to building empirical equations to calculate one component of a tree by measuring another (e.g., determining above-ground biomass from crown length, Kantola and Mäkelä, 2006). As the canopy represents the centre of photosynthesis and biomass production in a tree, obtaining a deeper understanding of its organisation is of particular interest in highly productive forest species, such as *Pinus radiata* D. Don. In the last decades, wood quality modelling based on tree development processes and crown architecture has increased. For instance, Mäkelä and Mäkinen (2003) presented a process-based tree and stand growth model to predict the stem structure with a 3D geometry and its internal knots, in Scots pine (*Pinus sylvestris* L.). In this study, statistical models were used to create individual branch information from the vertical profile of branch basal area. Ikonen et al. (2003) also demonstrated how Scots pine tree stem properties were linked to the properties of sawn timber. Particularly they concentrated on branch growth and distribution in the crown (and the corresponding knottiness of the sawn wood) and the influence of local light conditions on their attained size. Kantola et al. (2007) adapted an existing process-based growth model, PipeQual, to Norway spruce (*Picea abies* [L.] Karst.); it describes stand development and timber properties (stem taper, heartwood formation and branchiness). The model includes a branch module that calculates the annual dynamics of individual branches and their properties in each whorl. All calculations in the branch module are based on empirical, stochastic models that use tree and whorl level variables as input. Following the same research line, Lyhykäinen et al. (2009) developed models for estimating yields of lumber grades and by-products of individual Scots pine trees using stem and crown dimensions as explanatory variables. The model uses a data set simulated by a process-based growth model, which provides information about stem form and branch properties. The simulated stems are sawn using the WoodCim sawing simulator that grades the individual sawn pieces, as well as by-products. For other conifers as Douglas fir (*Pseudotsuga menziesii*) Hein et al. (2008) modelled branch number, diameter of the thickest branch and the relative branch diameter in the cluster, using non-linear models. As independent variables they used site index, relative height of the cluster, height diameter ratio and tree diameter at breast height among others. Weiskittel et al. (2010) modelled the number of branches/m of crown, maximum branch diameter in the crown and relative distribution of branch size within the crown for five conifers. Particularly, this study highlighted the range of variability in key crown structural attributes.

*P. radiata* is the main species involved in forestry industry in Australia, Chile and New Zealand. The industrial and economic importance of this species in the last 30 years has stimulated intensive studies aimed at improving the productivity and the quality of its wood. Within a growing season, *P. radiata* species may produce one growth unit per year on the main stem or multiple units in a polycyclic sequence (Fernández, 1994; Grace et al., 1998), and they are therefore considered polycyclic species. The set of growth units produced during a single growing season makes up the annual shoot. The polycyclic behaviour of *P. radiata* has been demonstrated by many authors, such as Jacobs (1936), Fielding (1960), Bannister (1962), Bollmann and Sweet (1976) and Fernández et al. (2007), among others. However, some of these trees may occasionally produce only one growth unit along the main axis in some years. Nevertheless, in all cases, the growth units end with a cluster of branches or of branches and cones.

The branches of *P. radiata* and many other forest species whose branches develop within a cluster generally present varying degrees of vigour. Barthélémy et al. (1997) explained this phenomenon based on the principle of acrotony, whereby the greatest vigour of branches is observed in the distal part of a growth unit. According to Lauri (2007), acrotony is usually defined as an increase in vigour (e.g., in length, diameter, number of leaves) in the vegetative proleptic branches (from dormant buds) moving from the bottom to the top position of parental growth. In this case, the basal branches show less vigour than the last branches formed in the same cluster, showing a gradient of vigour from the bottom to the top of the cluster (Fig. 1). Pont (2001) demonstrated that this is the case in *P. radiata* branching. From the lower branch in a cluster to the largest one at the top, there is a short distance and a divergence angle. This angle has been observed in the phyllotaxis of many organs (e.g., leaves, branches, petals) and species, and in many cases, it is coincident with the golden angle, $\omega \approx 137.5$ (Prusinkiewicz and Lindenmayer, 1990). The ratio of this angle to its complement, $gr = \omega/(360 - \omega)$, corresponds to the golden ratio ($gr$), which is widely observed in nature. Pont (2001) demonstrated that the divergence angle of the branch primordia in *P. radiata* is coincident with $\omega$. There have been some attempts to use empirical models to describe the characteristics of *P. radiata* branches, and in some cases, the diameter of the largest branch in a cluster has been taken as a reference unit (e.g., Grace et al., 1998). Similarly, Woollons et al. (2002) modelled the internode length and branch characteristics of *P. radiata* in New Zealand using traditional variables employed in common forestry inventories as inputs, such as tree height, diameter at breast height and the basal area per hectare of the top 100 stems. Fernández et al. (2007) studied the evolution of branch number, among other architectural characteristics, of the species along its life span. Further, Fernández et al. (2011) developed a functional–structural model for the species, modelling branchiness, growth unit frequency as well as internode length throughout different site and stand density scenario, using functional and also some stochastic models.

Empirical models are most commonly used to reflect the nature, but they do not completely reflect the real response of the studied tree/branch variables, that depend not only on site and tree structural considerations (site index, stand density, relative position of the branches in the crown, tree dominance) but also on natural stochastic events that might be affecting the tree and its components development. As stated by Barthélémy and Caraglio (2007) the architecture of a plant arises from the balance between the expression of the endogenous growth process and exogenous constraints conferred by the environment. Thus, the original architectural plan or model can take multiple expressions that a deterministic modelling approach do not represent, because by definition, it gives a unique response value under certain input. But the unpredictable events might be affecting directly or indirectly (for instance their neighbours) the modelled subject (for us a branch), generating variations in their expected relative vigour (given by acrotony). In the seek of modelling natural phenomena and its variability, we propose stochastic modelling which permits to capture the rich variability that is normally observed in nature, and particularly Markov chains, that have been used successfully to model tree architecture (branching, shoot structure, flowering, for instance) as can be seen in Guédon et al. (2001) and Guédon et al. (2007).

According to Gilks et al. (1996), Markov chains represent stochastic processes in discrete time and discrete events that undergo a transition from one state to another among a finite number of possible states. They are built from simple dependencies between successive random variables, and thus, the transition from

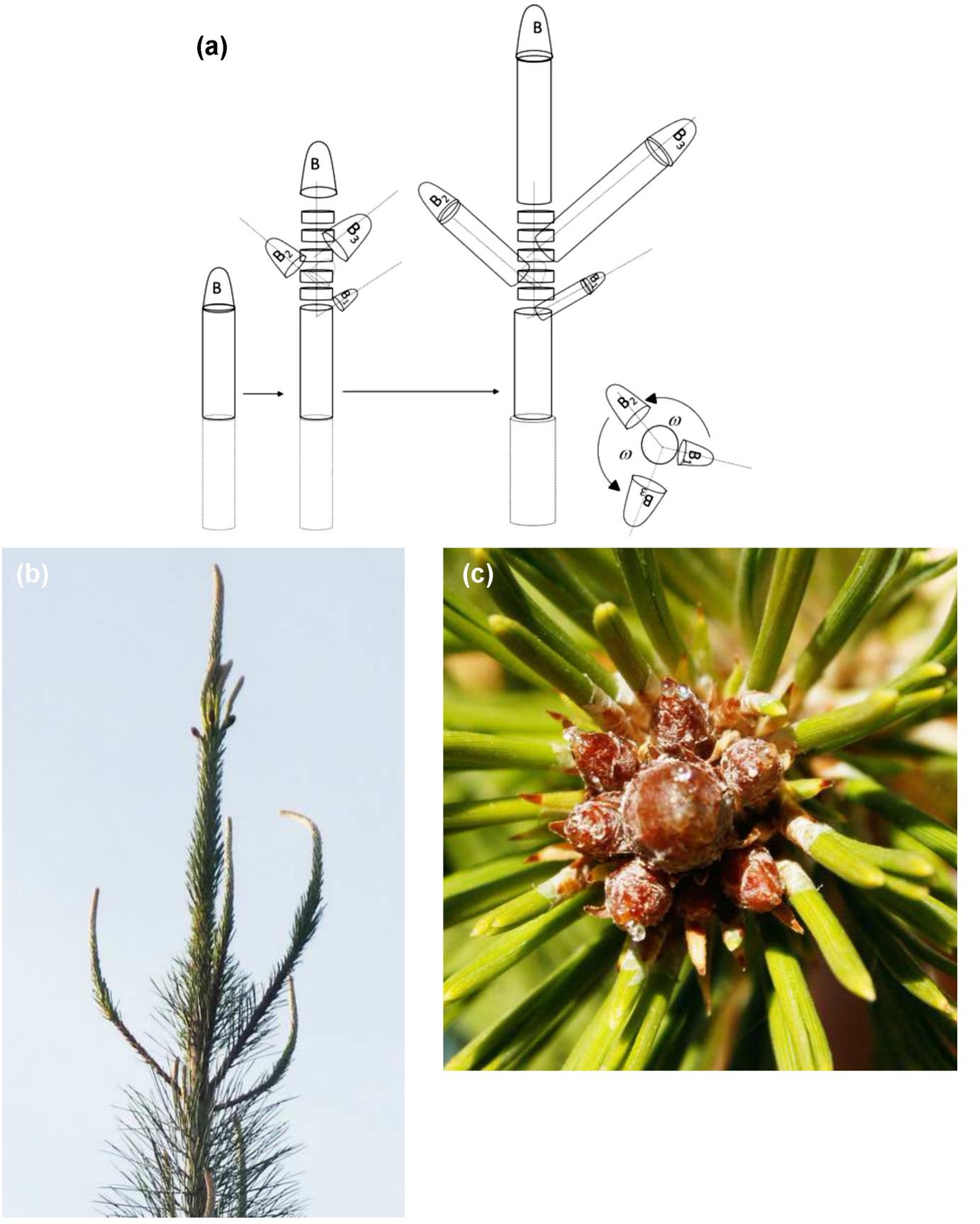


**Fig. 1.** (a) Schema of the arrangement of buds/branches as well as their vigour in a cluster and the $\omega$ divergence angle between two consecutive branches in the horizontal plane; (b) a developing cluster of branches of *Pinus radiata* and (c) a bud cluster view from the top.

**Table 1**
Characteristics of the stands and material.

| | Los Alamos | | Santa Gertrudis | La Granja | San Martín |
|---|---|---|---|---|---|
| Location | 37° 40′ 2″ S | 73° 3′ 13″ W | 37° 23′ 8″ S 72° 47′ 50″ W | 37° 54′ 38″ S 72° 24′ 24″ W | 34° 41′ 41″ S 71° 47′ 39″ W |
| | Stand 1 | Stand 2 | Stand 1 | Stand 1 | Stand 1 |
| Site index (age 20) | 34 | 34 | 28 | 27 | 22 |
| Planting year | 1998 | 1987 | 1997 | 1988 | 2000 |
| Age | 5 | 16 | 6 | 15 | 9 |
| Stand density (trees/ha) | 1250 | 1200 | 1250 | 1100 | 1117 |
| Sampled trees | 26 | 20 | 20 | 20 | 39 |
| Mean height (m) | 5.26 (0.6) | 24.2 (2.3) | 5.17 (1.24) | 19.0 (2.2) | 8.6 (2.0) |
| Mean DBH (cm) | 7.58 (1.29) | 24.5 (5.2) | 6.3 (2.4) | 21.3 (5.48) | 10.6 (1.5) |

*Note*: average values accompanied by standard deviation in brackets.

state *i* to a state *j* depends only on the current state, *i*, and not on the sequence of events that preceded it.

Our hypothesis is that *P. radiata* branches present acrotony within a cluster that is later modulated by stochastic events, such as local light conditions and the interactions with the nearest branches. We choose Markov chain stochastic modelling because we think it is particularly suitable for modelling both phenomena simultaneously; acrotony but also the stochastic alteration of the original programme. The interaction between successive branches expressed as the intrinsic acrotony of the species get modelled when assuming that a branch is followed by a smaller one from the top to the base of the cluster. Thus, for example the size of a certain branch from top to base gives the following branch a size limit: it can be equal or smaller. But by the other hand, the inclusion of a probability distribution of being smaller at different scales includes stochasticity that generates variability in the branching process. In our case, the model that we propose implies that within a cluster of branches, the relative vigour of a branch depends on the relative vigour of its prior neighbouring branch. Thus, there will be a probability of moving from state *i* (the state of a branch) to state *j* (the state of the following branch in the cluster), giving the stochastic chance to the second branch to be equal or smaller than the previous one. Thus, the main objective of this research is to develop a method to describe the relative branch size transition within a cluster that incorporates both the effect of acrotony and the stochastic variability that is commonly observed in nature.

## 2. Materials and methods

### 2.1. Materials

For this study, a total of 125 individual trees were examined from four different geographical locations and five age categories: 5, 6, 9, 15 and 16 years of age (Table 1). The inclusion of different ages is useful to better understand the pattern of development of the trees, as young trees may show early characteristics that are difficult to detect in older trees, whereas mature trees may reveal later-developing features that are not present in juvenile stages. All of the selected stands were unmanaged.

Broken and damaged trees were excluded from the measurements because of their irregular canopy growth. The relevant measured architectural parameters were total tree height and diameter at breast height; the length of each growth unit and the base diameter of every growth unit; the number of branches, cones and buds at each cluster; and the diameter and length of lateral branches. From the 125 individuals examined, a total of 2704 clusters of branches were included in further analyses.

### 2.2. Methods

#### 2.2.1. Data collection and analysis

First, a visual exploratory analysis of the whole dataset based on histograms and graphs was performed to obtain the general patterns of different relationships among the measured tree parameters. Based in the literature, several empirical models were tested as possible metrics for explaining the branch characteristics of our dataset (e.g., Grace et al., 1999; Kantola et al., 2007).

During the analysis of the architecture of *P. radiata*, the branches in each cluster were measured and their diameter was taken as an index of vigour. Thus, we assumed that their vigour depended on the principle of acrotony within the cluster, particularly at the stage of buds and emerging new branches (Fig. 1a and b), modified by posterior circumstances.

Next, the diameters of the branches in each cluster were ranked from the largest (most vigorous) to the smallest (less vigorous), and the absolute diameter values were transformed into relative values ($\upsilon$), defined as the ratio between the particular diameter of a branch ($d_i$) and the diameter of the largest branch ($d_{max}$) in a given cluster, $\upsilon = d_i/d_{max}$. Therefore, any cluster always exhibits a branch with $\upsilon = 1$ and branches with equal or gradually decreasing values of $\upsilon$ ($\upsilon \leq 1$).

Consequently, the following decision was made regarding modelling: the relative vigour of the branches in a cluster were divided into five groups or states: state 1 or $E_1$, $\upsilon$ [1,0.8); state 2 or $E_2$, $\upsilon$ [0.8, 0.6); state 3 or $E_3$, $\upsilon$ [0.6, 0.4); state 4 or $E_4$, $\upsilon$ [0.4, 0.2), and state 5 or $E_5$, $\upsilon$ [0.2, 0.0). This means that if a branch exhibits, for instance, a diameter between 40 and 60% of the diameter of the largest branch, this branch will be categorised as state 3. We chose to divide the relative vigour of branches in five states because a higher resolution was impractical and did not report more benefits for modelling purposes.

The clusters or whorls were grouped according to the number of branches in each of them. This decision was taken because the probability of transition from one state to another was different if the cluster had different number of branches, as preliminary data survey showed. Thus, individual probability matrix should be build for each type of cluster. All clusters with 3–12 branches were included in further analyses (i.e., they were a total of 10 cluster types). Although there were clusters with more than 12 branches (up to 27), they were rare, and in most cases, they corresponded to clusters that had suffered some traumatic event, making them very different from regular branches. Therefore, they were discarded from further analysis.

Finally, we assumed that within a cluster (i) we could sort the branches according to their relative vigour assuming an order based on the acrotony of the branches; (ii) the vigour of a branch would depend on the vigour of its prior neighbour (Fig. 1); (iii) although the order of appearance of the branches in the cluster is from

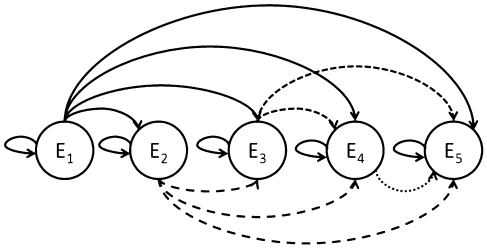


**Fig. 2.** Markov chain schema. All of the transitions from one state to another (connectors) exhibit a value of $0 \leq p_{ij} < 1$ for all i < j, and all states from $E_1$ to $E_4$ show a $p_{ii} < 1$, meaning that following a branch of certain vigour, there is a probability of another branch of the same vigour occurring. In the case of state $E_5$, there is a probability of $p_{55} = 1$ of remaining in the same state (the lowest one), corresponding to an absorbent state.

the bottom to the top (thus, the first to emerge are the smallest ones), they are formed almost simultaneously in the bud; and (iv) therefore, the vigor of a branch also depends on the vigor of a neighbor that is larger and appeared after it. Given these four assumptions, we decided to model the relative branch vigour as first-order Markov chains.

### 2.2.2. Markov chain

Once the 5 states and the 10 types of cluster (from 3 to 12 branches) were defined, a Markov chain transition matrix for each type of cluster was built. For the present study, the transition matrix $P_n$ (with $n$ number of branches per cluster) (Eq. (1)) was defined as the probabilities $p_{ij}$, of moving from state $E_i$ to state $E_j$, subject to the condition that $p_{ij} = 0$ if $i > j$, as branches are ranked from larger to smaller sizes. It means that if there is a branch of size $X$ that belong to a state $E_i$ (for instance $E_2$ of relative vigour $\upsilon$ [0.8, 0.6)), there is a probability $p_{ij}$ for the next branch top down in the cluster to be in the same state $E_i$; means equal in size to the previous one (in the example $p_{22} \geq 0$), or smaller ($p_{23} \geq 0$, $p_{24} \geq 0$, $p_{25} \geq 0$) but the next branch cannot be larger then the previous one ($p_{21} = 0$). For matrix calculations, 80% of the total dataset was used and 20% was used for validation. The selection of the datasets for the matrix calculation and validation was randomly done.

$$P_n = \begin{bmatrix} P_{11} & P_{12} & P_{13} & P_{14} & P_{15} \\ P_{21} & P_{22} & P_{23} & P_{24} & P_{25} \\ P_{31} & P_{32} & P_{33} & P_{34} & P_{35} \\ P_{41} & P_{42} & P_{43} & P_{44} & P_{45} \\ P_{51} & P_{52} & P_{53} & P_{54} & P_{55} \end{bmatrix} = \begin{bmatrix} P_{11} & P_{12} & P_{13} & P_{14} & P_{15} \\ 0 & P_{22} & P_{23} & P_{24} & P_{25} \\ 0 & 0 & P_{33} & P_{34} & P_{35} \\ 0 & 0 & 0 & P_{44} & P_{45} \\ 0 & 0 & 0 & 0 & P_{55} \end{bmatrix} \quad (1)$$

with $p_{ij} = 0$ if $i > j$.

When analysing the structure of the Markov chains, we observed that $E_j$ was only accessible from a state of $E_i$ if $i \leq j$. This means that the states were not communicated because even if $E_j$ was accessible from $E_i$ (for $i \neq j$), $E_i$ was not accessible from $E_j$. Thus, the Markov chains could be classified as reducible. All states were transitory (for $i < 5$), and the last state $E_5$, was absorbent; thus, the chains were absorbing Markov chains. When a branch displayed the lowest vigour ($E_5$), the following branches exhibit the same state ($E_5$), which means that once the system was in $E_5$, it is impossible to abandon it (Fig. 2):

$$P(X_k = E_5 | X_{k-1} = E_5) = 1.$$

The Markov chains were also irregular because all of the transition matrixes could present 0 (zero) values at any times.

### 2.2.3. Statistical analysis

Considering the cumulative probability transition matrixes, 300 stochastic simulations based on a Monte Carlo procedure were performed to create new data synthetically for each type of cluster. To guarantee the validity of the transition matrixes, the simulated dataset and the validation dataset (20% of the original dataset) were compared. Basic statistical analyses (e.g., calculation and comparison of means and standard deviations) and comparisons of probability distributions were carried out. The normality of the data distribution was tested, and because the hypothesis of normality was rejected for all clusters, non-parametric tests were selected for performing appropriate comparisons between the simulated and validation datasets. In this case, the Kolmogorov–Smirnov (K–S) was used because it is a goodness-of-fit test that assesses the uniformity of a set of data distributions. The null hypothesis was that the data and the validation dataset were drawn from the same distribution, against the alternative hypothesis that the two distributions differed. The exact K–S procedure was also conducted because it is the best procedure whenever it is practically possible to compute it (van de Wiel, 2002). The K–S test subtracts the most positive and negative differences between the two cumulative distribution functions that are being compared, with the highest sensitivity being observed around the median value (Stephens, 1970). To achieve a more complete comparison of the distributions, Kuiper's test was used, which compares the tails of the two probability distributions in addition to the median value. The $p$-value obtained in Kuiper's test refers to the probability of observing a larger value of the asymptotic Ka (value calculated by the test) under the null hypothesis of no difference between the two distribution classes (SAS Institute Inc., 2009). For the non-parametric statistical analyses, the PROC NPAR1WAY procedure of SAS (SAS Institute Inc., 2011) was used.

## 3. Results

More than the 50% of the clusters contained 5–7 branches. The mean number of branches was 6 (standard deviation 2.48), and the mode was also 6 ($n = 2704$ clusters) (Fig. 3a).

The distribution of the relative branch sizes was variable, depending on the numbers of branches per cluster (Fig. 3b). In general, there were few branches within the smallest size class $E_5$ (branches with relative size between 0 and 0.2). On average, clusters with 6–9 branches tended to have display balanced branch size distributions, while clusters with more branches accumulated relatively more small branches. Nevertheless, when individual clusters were examined, the distributions did not follow a common pattern, as observed in Fig. 4(a, c and e) for clusters with 4, 6 and 9 branches. This variability supported the need for stochastic modelling, and our choice of first-order Markov chains was partly supported by this finding.

One probability matrix was developed per branch cluster type (B3–B12) (Table 2). The Markov probability matrix showed the probability of a branch in state $E_i$ of being followed by a branch in state $E_j$, subject to the condition that $p_{ij} = 0$ if $i > j$, as branches are ranked from larger to smaller sizes. Thus, to summarise the characteristics of the obtained matrix, (a) $p_{ii} > 0$ for $i \leq 4$; (b) $p_{ii} = 1$ for $i = 5$; (c) $0 \leq p_{ij} < 1$ for all $i < j$; and (d) $p_{ij} = 0$ for all $i > j$. This means that a branch of a certain size can be followed by another branch of the same vigour or smaller, whereas a branch of the smallest size (vigour state $E_5$) can only be followed by a branch of the same vigour state, $E_5$. In matrixes with a small number of branches (B3–B5), there was always a probability of a branch being followed by a smaller branch from any of the other states. However, in clusters with larger number of branches (B6–B12), the probability of a large branch to be followed by a very small one could be 0 (Table 2).

**Table 2**
First-order Markov probability matrixes for branch vigour. Vigour state 1, $E_1$, $\upsilon$ [1,0.8); vigour state 2, $E_2$, $\upsilon$ [0.8, 0.6); vigour state 3, $E_3$, $\upsilon$ [0.6, 0.4); vigour state 4, $E_4$, $\upsilon$ [0.4, 0.2); and vigour state 5, $E_5$, $\upsilon$ [0.2, 0.0); with (Bn: cluster with *n* branches).

| **B3** | 1 | 0.8 | 0.6 | 0.4 | 0.2 | **B4** | 1 | 0.8 | 0.6 | 0.4 | 0.2 | **B5** | 1 | 0.8 | 0.6 | 0.4 | 0.2 |
|---|---|---|---|---|---|---|---|---|---|---|---|---|---|---|---|---|---|
| 1 | 0.41 | 0.32 | 0.15 | 0.1 | 0.02 | 1 | 0.49 | 0.31 | 0.13 | 0.06 | 0.01 | 1 | 0.54 | 0.34 | 0.08 | 0.03 | 0.01 |
| 0.8 | 0 | 0.3 | 0.46 | 0.18 | 0.05 | 0.8 | 0 | 0.35 | 0.41 | 0.19 | 0.05 | 0.8 | 0 | 0.48 | 0.35 | 0.13 | 0.04 |
| 0.6 | 0 | 0 | 0.52 | 0.28 | 0.2 | 0.6 | 0 | 0 | 0.4 | 0.46 | 0.13 | 0.6 | 0 | 0 | 0.49 | 0.4 | 0.11 |
| 0.4 | 0 | 0 | 0 | 0.78 | 0.22 | 0.4 | 0 | 0 | 0 | 0.59 | 0.41 | 0.4 | 0 | 0 | 0 | 0.61 | 0.39 |
| 0.2 | 0 | 0 | 0 | 0 | 1 | 0.2 | 0 | 0 | 0 | 0 | 1 | 0.2 | 0 | 0 | 0 | 0 | 1 |
| **B6** | 1 | 0.8 | 0.6 | 0.4 | 0.2 | **B7** | 1 | 0.8 | 0.6 | 0.4 | 0.2 | **B8** | 1 | 0.8 | 0.6 | 0.4 | 0.2 |
| 1 | 0.57 | 0.33 | 0.08 | 0.02 | 0 | 1 | 0.6 | 0.32 | 0.06 | 0.02 | 0 | 1 | 0.64 | 0.3 | 0.05 | 0.01 | 0 |
| 0.8 | 0 | 0.47 | 0.36 | 0.13 | 0.04 | 0.8 | 0 | 0.52 | 0.37 | 0.09 | 0.01 | 0.8 | 0 | 0.56 | 0.35 | 0.09 | 0.01 |
| 0.6 | 0 | 0 | 0.51 | 0.42 | 0.07 | 0.6 | 0 | 0 | 0.55 | 0.4 | 0.05 | 0.6 | 0 | 0 | 0.57 | 0.39 | 0.04 |
| 0.4 | 0 | 0 | 0 | 0.79 | 0.21 | 0.4 | 0 | 0 | 0 | 0.72 | 0.28 | 0.4 | 0 | 0 | 0 | 0.72 | 0.28 |
| 0.2 | 0 | 0 | 0 | 0 | 1 | 0.2 | 0 | 0 | 0 | 0 | 1 | 0.2 | 0 | 0 | 0 | 0 | 1 |
| **B9** | 1 | 0.8 | 0.6 | 0.4 | 0.2 | **B10** | 1 | 0.8 | 0.6 | 0.4 | 0.2 | **B11** | 1 | 0.8 | 0.6 | 0.4 | 0.2 |
| 1 | 0.62 | 0.31 | 0.06 | 0.01 | 0 | 1 | 0.64 | 0.31 | 0.04 | 0 | 0 | 1 | 0.62 | 0.36 | 0.02 | 0 | 0 |
| 0.8 | 0 | 0.61 | 0.34 | 0.06 | 0 | 0.8 | 0 | 0.65 | 0.3 | 0.05 | 0 | 0.8 | 0 | 0.63 | 0.31 | 0.06 | 0 |
| 0.6 | 0 | 0 | 0.6 | 0.37 | 0.04 | 0.6 | 0 | 0 | 0.54 | 0.43 | 0.03 | 0.6 | 0 | 0 | 0.52 | 0.46 | 0.01 |
| 0.4 | 0 | 0 | 0 | 0.78 | 0.22 | 0.4 | 0 | 0 | 0 | 0.72 | 0.28 | 0.4 | 0 | 0 | 0 | 0.81 | 0.19 |
| 0.2 | 0 | 0 | 0 | 0 | 1 | 0.2 | 0 | 0 | 0 | 0 | 1 | 0.2 | 0 | 0 | 0 | 0 | 1 |
| **B12** | 1 | 0.8 | 0.6 | 0.4 | 0.2 | | | | | | | | | | | | |
| 1 | 0.59 | 0.41 | 0 | 0 | 0 | | | | | | | | | | | | |
| 0.8 | 0 | 0.58 | 0.39 | 0.03 | 0 | | | | | | | | | | | | |
| 0.6 | 0 | 0 | 0.65 | 0.32 | 0.03 | | | | | | | | | | | | |
| 0.4 | 0 | 0 | 0 | 0.86 | 0.14 | | | | | | | | | | | | |
| 0.2 | 0 | 0 | 0 | 0 | 1 | | | | | | | | | | | | |

For instance, for B6 clusters, large branches (state $E_1$) were not followed by the smallest branches with vigour of 0.2 (state $E_5$). In general, the greater the number of branches in a cluster, the lower the probability that a large branch is followed by a very small one (Table 2).

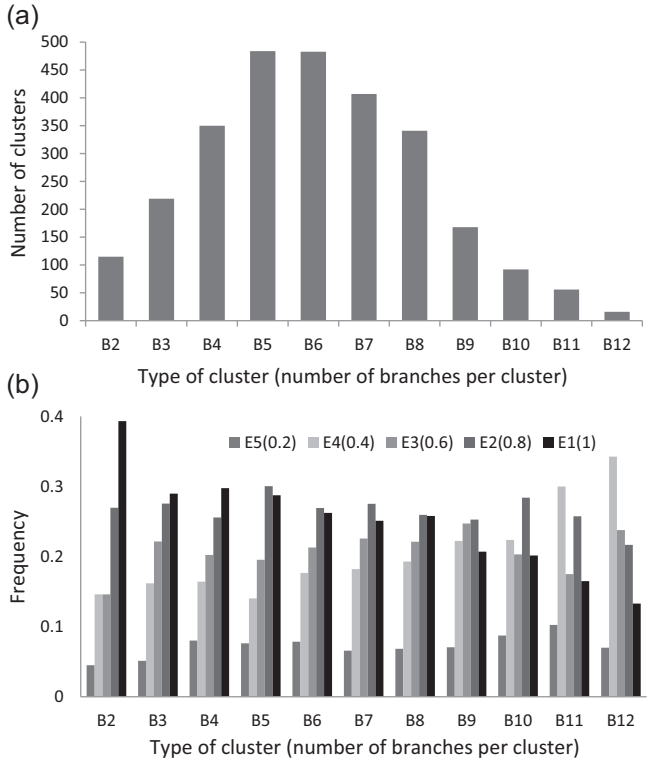


**Fig. 3.** (a) Frequency of number of branches per cluster, with an average value of 6. (b) Observed mean relative branch size distribution per cluster (Bn = clusters with n branches) (right). Relative sizes: 0.2 [1, 0.8), 0.4 [0.8, 0.6), 0.6 [0.6, 0.4), 0.8 [0.4, 0.2) and 1 [0.2, 0.0).

The initial distribution would always be $q_o = (1\,0\,0\,0\,0)$, meaning that the initial state of the sequence of branches will be always the highest state ($E_1$). The limit distribution, $q_l = q_0 \cdot P^T$, when $T$ = Bn (Bn, the branch number for the different types of clusters) would be as shown in Table 3. The limit distribution was calculated considering that the horizon of calculation depends on the number of branches. However, if we consider a limit distribution where $T \to \infty$, it will correspond to $q_l = (0\,0\,0\,0\,1)$.

A Monte Carlo simulation process was followed to generate a new dataset based on the observed probabilities shown in Table 2. The generated dataset was tested against the validation dataset using the non-parametric Kolmogorov–Smirnov (K–S) test as well as Kuiper's test (van de Wiel, 2002; SAS Institute Inc., 2009). No significant values were obtained for any of the probability distributions (Table 4), meaning that the generated data and validation data showed the same probability distribution (Fig. 5, Table 4) and, thus, could be considered as the same.

## 4. Discussion

The frequency distribution of the number of branches per cluster showed a mean and a mode of 6 branches. Similar results were obtained in other studies, where a mode between 5 and 8 branches

**Table 3**
Limit distribution of the different types of clusters with B3–B12 branches. $E_{1-5}$, vigour states.

| | $E_1$ (1) | $E_2$ (0.8) | $E_3$ (0.6) | $E_4$ (0.4) | $E_5$ (0.2) |
|---|---|---|---|---|---|
| B3 | 0.07 | 0.12 | 0.28 | 0.31 | 0.22 |
| B4 | 0.06 | 0.09 | 0.18 | 0.31 | 0.35 |
| B5 | 0.05 | 0.12 | 0.18 | 0.27 | 0.38 |
| B6 | 0.03 | 0.08 | 0.15 | 0.40 | 0.34 |
| B7 | 0.03 | 0.07 | 0.15 | 0.33 | 0.41 |
| B8 | 0.03 | 0.07 | 0.14 | 0.32 | 0.46 |
| B9 | 0.01 | 0.06 | 0.13 | 0.36 | 0.47 |
| B10 | 0.01 | 0.06 | 0.09 | 0.26 | 0.55 |
| B11 | 0.01 | 0.04 | 0.06 | 0.36 | 0.53 |
| B12 | 0.00 | 0.01 | 0.07 | 0.41 | 0.51 |

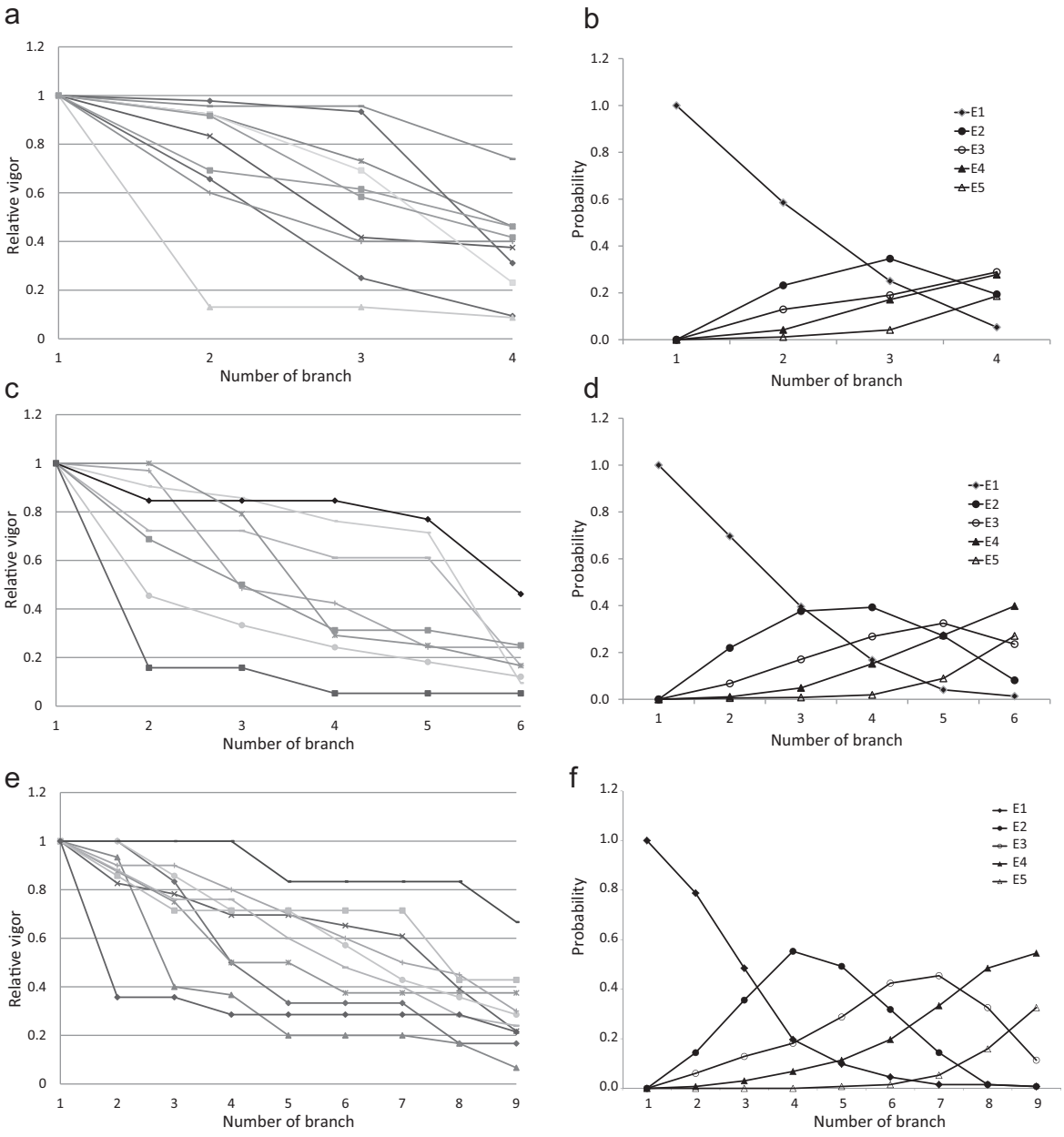


**Fig. 4.** Examples of vigour relationships between branches of a cluster based on their basal diameter; (a) each line corresponds to randomly selected clusters of 4 branches, (c) of 6 branches and (e) of 9 branches. In parallel, the probability of each type of branch vigour (E1–E5) among the different branches is shown for clusters of (b) 4 branches, (d) 6 branches and (f) 9 branches.

was observed among *P. radiata* trees in New Zealand (Madgwick, 1994; Grace et al., 1999; Woollons et al., 2002). When we compared the frequency distributions of the number of branches per cluster in our data with those of Grace et al. (1999) (for *P. radiata* trees grown in New Zealand) using the Kolmogorov–Smirnov test for two populations (hypothesis H0: the two populations are the same), the resultant *p*-value was 0.06, meaning that there was no real evidence rejecting the null hypothesis. This is an interesting result, considering that the only common point in the two datasets is the tree species. Site conditions were different between the New Zealand and Chilean sites, as were the management regimes and tree ages. Thus, this result could indicate that the number of branches per cluster is a strong species-specific characteristic, though modulated by environmental conditions.

Madgwick (1994) studied the acrotony of the branches in *P. radiata* and concluded that between two consecutive branches, there was a decrease of 12% in diameter size on average. However, in the present study, such a clear pattern was not found. For instance, Fig. 4 illustrates the large variability observed in branch vigour sequences in the clusters, indicating that there was no such pattern being followed. At one extreme, there were clusters whose branches were all of similar vigour, while at the other extreme, a remarkable gradient could be observed between branches. Grace et al. (1999) also found that *P. radiata* branch diameter varies considerably within a cluster. These various combinations might be due to initial acrotony at the time of the generation of the cluster, followed later by the elimination of this early influence because of competition for light or metabolites or due to accidental events that have taken place throughout the life span of the branches, prior to the time of measurements.

There have been many attempts to model branch numbers and characteristics using empirical models (e.g., Mäkinen and

**Table 4**
Kolmogorov–Smirnov (K–S) and Kuiper two-sample test. Values of Pr < 0.05 indicate differences between the validation and generated datasets.

| | K-S two sample test | | Kuiper Two-Sample Test | |
|---|---|---|---|---|
| | Pr > *D* | Exact Pr ≥ *D* | Ka | Pr > Ka |
| B3 | 0.996 | 0.730 | 0.410 | 1.000 |
| B4 | 0.417 | 0.136 | 0.883 | 0.936 |
| B5 | 0.220 | 0.060 | 1.050 | 0.756 |
| B6 | 0.312 | 0.102 | 1.337 | 0.344 |
| B7 | 0.203 | 0.057 | 1.222 | 0.502 |
| B8 | 0.674 | 0.272 | 1.302 | 0.389 |
| B9 | 0.186 | 0.051 | 1.090 | 0.700 |
| B10 | 0.700 | 0.291 | 0.919 | 0.908 |
| B11 | 0.992 | 0.723 | 0.433 | 1.000 |
| B12 | 0.771 | 0.309 | 1.062 | 0.740 |

Colin, 1998; Grace et al., 1998, 1999; Trincado and Burkhart, 2009; Weiskittel et al., 2010). As an initial test, in the present study, we intended to model the relative size of the branches in our dataset following an empirical model presented by Grace et al. (1999), in which the relative diameter size was dependent on *n*: the rank of the branch in the cluster when ranked by the diameter from largest to smallest. However, as expected, the results were very poor because of the variability in the relative branch size distributions (see Fig. 4). In addition to other branch characteristics, the number of branches per cluster was modelled (e.g., following the equation reported by Kantola et al., 2007), but very poor outcomes were also obtained in this case. Therefore, the poor results of the tested empirical models regarding branch characteristics, the variability of the branch size distributions, and the acrotony of *P. radiata* branches documented by Pont (2001) and by us in newly forming branches (unpublished data) were decisive in the choice to follow the stochastic approach we took using a Markov process. Theoretically, our methodology is assuming initial branch development (in the bud stage) with marked acrotonic behaviour and posterior stochastic evolution, considering the particular conditions each branch can experience during its lifespan. Our assumption that the original acrotonic behaviour can be altered by subsequent differences in the environment within the same cluster is consistent with the results of Grace et al. (1999), who observed a tendency of larger branches in the side of the trees facing north in *P. radiata* in New Zealand.

When observing the transition matrix (Table 2), it is evident that between similar clusters (for example, a cluster with 4 branches and a cluster with 5 branches), there is a similar probability of transitioning from state *i* to a state *j*. However, when observing all of the obtained transition matrixes, a gradient is evident. For example, from cluster with 3 to clusters with 8 branches, the transition probability from $E_1$ to $E_2$ increases continuously from 0.41 to 0.64, then becomes relatively stable at approximately 0.62. Thus, for modelling purposes, we consider it to be appropriate to work with an independent transition matrix for each type of cluster, instead of a unique transition matrix constructed with all of the clusters.

The results of the comparison between the validation and the simulated datasets (Table 4 and Fig. 5) indicate that the selected stochastic approach for relative branch size simulation within a cluster is a reliable method. As a modelling approach, we suggest (i) simulation of the number of branches (NB) in a cluster according to the observed distribution (Fig. 3); (ii) simulation of the relative sizes of the NB using Monte Carlo and the transition matrix; (iii) re-scaling of the relative sizes of the branches to the real sizes based on the largest branch diameter (model not proposed in this paper); and (iv) finally, for 3D modelling purposes, arranging the branches in a spiral phyllotaxis from the smallest to the largest branch in the cluster, with a vertical distance of *d* between the insertion point of the branches and a divergence angle of $\omega \approx 137.5^\circ$ (Fig. 1).

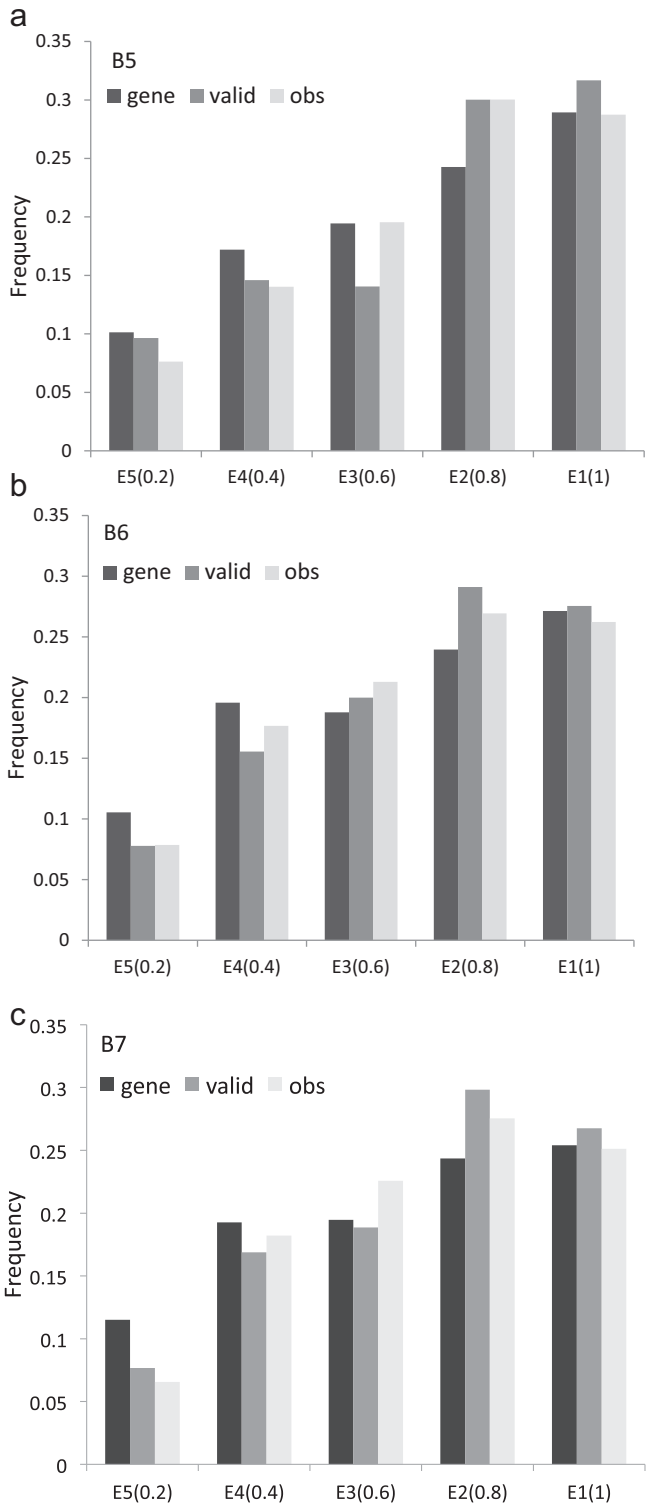


**Fig. 5.** Examples of branch vigour frequencies for clusters with (a) 5, (b) 6 and (c) 7 branches (B5–B7). Averages for the datasets used for calibration (obs), for validation (valid) and the predicted (gen) datasets.

## 5. Conclusions

The main aim of this investigation was to define the acrotony of the branches in a branch cluster in *P. radiata*, using Markov chain process. Finally, we concluded that the proposed method permits to simulate simultaneously the expected acrotony of branches for the species but modulated by stochastic events, giving special weight to

the relationship between a branch and its neighbours in the cluster. With the proposed method the use of relative size of the branches allows to utilise the method with different modelling approaches (e.g., functional–structural plant models, empirical models). No matter the model used to generate the number of branches in the cluster and the diameter of the largest branch of the cluster, then the rest of the branches sizes are re-scaled according to the results obtained by the Markovian simulation. As there already exist many models in the reviewed literature that generates the largest diameter of branches along the stem, our proposed approach could be coupled easily to them, in order to give a more realistic branches diameter distribution inside of the clusters.

The proposed method might be very useful in empirical models of the type presented by Maguire et al. (1994) or by Mäkinen et al. (2003) describing branch characteristics by multivariate methods; or in models like the one presented by Mäkinen and Mäkelä (2003) or Kantola et al. (2007) that consider a stochastic distribution of branch size within a whorl but based on an uniform distribution that do not reflect the acrotony of branches. It might also be useful in wood quality models, extensively reviewed in Mäkelä et al. (2010), because branch size distribution has an important effect on knottiness and final value of wood products. But particularly, it could be beneficial in functional–structural models or models that integrate physiological process with the corresponding plant structure relation, already stressed by different authors like Fourcaud et al. (2008) in their review on modelling approaches, or in carbon allocation modelling strategies as reviewed in Mäkelä (2012).

In the near future, the presented method should be integrated in functional–structural modelling following the approach suggested by Fernández et al. (2011); when a new cluster is generated, the relative size of the simulated branches permits appropriate and differentiated carbon allocation for the forming branches, immediately generating a non-homogeneous cluster, as observed in nature. The methodology tested here using data from *P. radiata* could be applied to other species just by determining the probability matrixes of the other species. Thus, it would also be interesting to apply the presented method to other *P. radiata* trees grown in other locations as well as to other species that follow the branch acrotony and to observe if the Markov chain probabilities differ.

## Acknowledgments

This research and publication were partially financed by Chilean FONDECYT Project Number 11085008 and by the Marie Curie Action ForEAdapt project funded by the European Union Seventh Framework Programme (FP7-PEOPLE-2010-IRSES) under Grant Agreement No. PIRSES-GA-2010-269257. A.Z.G. would also like to acknowledge the financial support of the FCT (SFRH/BPD/63979/2009) and the UEF foundation (project 930341).

## References

Bannister, M.H., 1962. Some variations in the growth pattern of *Pinus radiata* in New Zealand. New Zealand Journal of Science 5, 342–370.

Barthélémy, D., 2003. Botanical background for plant architecture analysis and modelling. In: Hu, B.-G., Jaeger, M. (Eds.), Proceedings PMA03. 2003 International Symposium of Plant Growth Modeling, Simulation, Visualization and Their Applications. Beijing, China, 13–26 October 2003, pp. 1–20.

Barthélémy, D., Caraglio, Y., 2007. Plant architecture: a dynamic, multilevel and comprehensive approach to plant form, structure and ontogeny. Annals of Botany 99 (3), 375–407.

Barthélémy, D., Caraglio, Y., Costes, E., 1997. Architecture, gradients morphogénétiques et age physiologique chez les végétaux. In: Bouchon, J., de Reffye, Ph., Barthélémy, D. (Eds.), Modélisation et simulation de l'architecture des végéteaux. INRA Editions, Paris, pp. 89–136.

Bollmann, M.P., Sweet, G.B., 1976. Bud morphogenesis of *Pinus radiata* in New Zealand. The initiation and extension of the leading shoot of one clone at two sites. New Zealand Journal of Forestry Science 6, 376–392.

Fernández, M.P., 1994. Arquitectura y modelación de árboles aplicada a Pino Insigne (*Pinus radiata* D. Don) (Architecture and tree modelling applied to Pino Insigne (*Pinus radiata* D. Don)). Universidad de Chile, Chile, Forest Engineer Degree Thesis (in Spanish).

Fernández, M.P., Norero, A., Barthélémy, D., Vera, J., 2007. Morphological trends in main stem of *Pinus radiata* D. Don: transition between vegetative and reproductive phase. Scandinavian Journal of Forest Research 22, 398–406.

Fernández, M.P., Norero, A., Vera, J., Pérez, E., 2011. A functional–structural model for radiata pine (*Pinus radiata*) focusing on tree architecture and wood quality. Annals of Botany 108, 1155–1178.

Fielding, J.M., 1960. Branching and flowering characteristics of Monterey pine. In: Bulletin Commonwealth Forest Timber Bureau Australia No. 37.

Fourcaud, T., Zhang, X., Stokes, A., Lambers, H., Körner, C., 2008. Plant growth modelling and applications: the increasing importance of plant architecture in growth models. Annals of Botany 101, 1053–1063.

Gilks, W.R., Richardson, S., Spigelhalter, D.J., 1996. Markov Chain Monte Carlo in Practice. Chapman Hall, London.

Grace, J.C., Blundells, W., Pont, D., 1998. Branch development in *Pinus radiata* – model outline and data collection. New Zealand Journal of Forestry Science 28 (2), 182–194.

Grace, J.C., Pont, D., Goulding, J., Brawley, B., 1999. Modeling branch development for forest management. New Zealand Journal of Forestry Science 29 (3), 391–408.

Guédon, Y., Barthélémy, D., Caraglio, Y., Costes, E., 2001. Pattern analysis in branching and axillary flowering sequences. Journal of Theoretical Biology 212, 481–520.

Guédon, Y., Caraglio, Y., Heuret, P., Lebarbier, E., Meredieu, C., 2007. Analyzing growth components in trees. Journal of Theoretical Biology 248, 418–447.

Hein, S., Weiskittel, A.R., Kohnle, U., 2008. Branch characteristics of widely spaced Douglas-fir in south-western Germany: comparisons of modelling approaches and geographic regions. Forest Ecology and Management 256, 1064–1079.

Ikonen, V.-P., Kellomäki, S., Peltola, H., 2003. Linking tree stem properties of Scots pine (*Pinus sylvestris* L.) to sawn timber properties through simulated sawing. Forest Ecology and Management 174, 251–263.

Jacobs, M.R., 1936. The detection of annual stages of growth in the crown of *Pinus radiata*. Part I: Morphological features of use in the recognition of annual stages of growth. Commonwealth Forest Bureau Bulletin Australia 19, 5–16.

Kantola, A., Mäkelä, A., 2006. Development of biomass proportions in Norway spruce (*Picea abies* [L.] Karst.). Trees 20, 111–121.

Kantola, A., Mäkinen, H., Mäkelä, A., 2007. Stem form and branchiness of Norway spruce as a sawn timber—predicted by a process based model. Forest Ecology and Management 241, 209–222.

Lauri, P.-E., 2007. Differentiation and growth traits associated with acrotony in the apple tree (*Malus domestica*, Rosaceae). American Journal of Botany 94 (8), 1273–1281.

Lyhykäinen, H.T., Mäkinen, H., Mäkelä, A., Pastila, S., Heikkilä, A., Usenius, A., 2009. Predicting lumber grade and by-product yields for Scots pine trees. Forest Ecology and Management 258, 146–158.

Madgwick, H.A.I., 1994. *Pinus radiata* – biomass, form and growth. Rotorua, 428pp.

Maguire, D.A., Moeur, M., Bennett, W.S., 1994. Models for describing basal diameter and vertical distribution of primary branches in young Douglasfir. Forest Ecology and Management 63, 23–25.

Mäkelä, A., 2012. On guiding principles for carbon allocation in eco-physiological growth models. Tree Physiology 32, 644–647.

Mäkelä, A., Mäkinen, H., 2003. Generating 3D sawlogs with a process-based growth model. Forest Ecology and Management 184, 337–354.

Mäkelä, A., Givnish, T.J., Berninger, F., Buckley, T.N., Farquhar, G.D., Hari, P., 2002. Challenges and opportunities of the optimality approach in plant ecology. Silva Fennica 36, 605–614.

Mäkelä, A., Grace, J.C., Deckmyn, G., Kantola, A., Campioli, M., 2010. Simulating wood quality in forest management models. Forest Systems 19 (SI), 48–68.

Mäkinen, H., Colin, F., 1998. Predicting branch angle and branch diameter of Scots pine from usual tree measurements and stand structural information. Canadian Journal of Forest Research 28, 1686–1696.

Mäkinen, H., Mäkelä, A., 2003. Predicting basal area of Scots pine branches. Forest Ecology and Management 179, 351–362.

Mäkinen, H., Ojansuu, R., Sairanen, P., Yli-Kojola, H., 2003. Predicting branch characteristics of Norway spruce (*Picea abies* (L.) Karst.) from simple stand and tree measurements. Forestry 76 (5), 525–546.

Monserud, R.A., Marshall, J.D., 1999. Allometric crown relations in three northern Idaho conifers species. Canadian Journal of Forest Research 29, 521–535.

Pont, D., 2001. Use of phyllotaxis to predict arrangement and size of branches in *Pinus radiata*. New Zealand Journal of Forestry Science 31, 247–262.

Prusinkiewicz, P., Lindenmayer, A., 1990. The Algorithmic Beauty of Plants. Springer-Verlag, New York, pp. 228.

SAS Institute Inc., 2009. SAS/STAT® 9.2 User's Guide, second edition. SAS Institute Inc., Cary, NC.

SAS Institute Inc., 2011. SAS® 9.3 System Options: Reference, second edition. SAS Institute Inc., Cary, NC, 340pp.

Stephens, M.A., 1970. Use of Kolmogorov–Smirnov, Cramer–von Mises and related statistics without extensive tables. Journal of the Royal Statistical Society 32, 115–122.

Todoroki, C.L., West, G.G., Knowles, R.L., 2001. Sensitivity analysis of log and branch characteristics influencing sawn timber grade. New Zealand Journal of Forestry Science 31, 101–119.

Trincado, G., Burkhart, H.E., 2009. A framework for modeling the dynamics of first order branches and spatial distribution of knots in loblolly pine trees. Canadian Journal Forest Research 39, 566–579.

van de Wiel, M.A., 2002. Exact Distributions of Distribution-free Test Statistics. Universiteitsdrukkerij Technische Universiteit Eindhoven, PhD thesis, 165pp.

Weiskittel, A.R., Seymour, R.S., Hofmeyer, P.V., Kershaw, J.A., 2010. Modelling primary branch frequency and size for five conifer species in Maine, USA. Forest Ecology and Management 259, 1912–1921.

Woollons, R.C., Haywood, A., Mcnickle, D.C., 2002. Modeling internode and branch characteristics for *Pinus radiata* in New Zealand. Forest Ecology and Management 160, 243–251.